Journal of Cleaner Production 368 (2022) 133005

Contents lists available at ScienceDirect

Journal of Cleaner Production

journal homepage: www.elsevier.com/locate/jclepro

Producing green Roller Compacted Concrete (RCC) using fine copper slag aggregates

Ehsan Sheikh, Seyed Roohollah Mousavi *, Iman Afshoon

Department of Civil Engineering, University of Sistan and Baluchestan, Zahedan, Iran

ARTICLE INFO

Handling Editor: M.T. Moreira

Keywords:
Copper slag aggregates
Green concretes
Compressive strength
Roller compacted concrete
SEM

ABSTRACT

Improving the concrete mechanical properties/durability indicators and reducing its costs and environmental damage by using waste materials have always been strategies for the growth and development of the concrete industry, waste management and environmental protection. This research studied the effects of using fine copper slag (CS) aggregates on the strength and microstructural properties of roller compacted concretes (RCC) by testing a total of 7 mix-designs including 0–60% fine copper slag aggregates and the results showed that the best compressive strength performance, about 23.58% more than that of the control design, was related to the 91-day concrete containing 40% CS. An increase in the CS increased the RCC's tensile and flexural strength. Different-age, 40% copper-slag specimens had the lowest surface and capillary water absorption and penetration rates, and 60% ones had about 7% increase in the unit weight and 26.8% reduction in the production costs. The mechanical properties were studied by scanning electron microscope (SEM) images and the results showed that this research can help collect copper slag waste from the nature, produce nature-friendly RCCs, reduce pollutants and waste depot spaces, save energy and preserve the environment.

1. Introduction

Producing one ton of pure copper produces about 2.2–3 tons of copper slag (CS) as a waste by-product that has high FeO_2 and low SiO_2, Al_2O_3 and CaO (Gorai et al., 2003), and is released into the nearby environment (Shi et al., 2008). In 2015, the major CS production was by China, Japan, Chile, Russia and India (about 56%) (Sharma and Khan, 2018), but such factors as the expansion of cities, population growth and urban development led to its more production compared to 2015; the average annual CS production is about 30 million tons which is stored in the nature often unused (Shen and Forssberg, 2003). From the environmental protection point of view, storage of this volume of waste in the nature is not justified due to high costs and environmental hazards as well as the required land and space (Khanzadi and Behnood, 2009). Although part of this waste is used in producing engineering materials (tiles, cement, glass, mortar, concrete, etc.), making abrasive/cutting tools and constructing roads, railways, airport runways, embankments and drainages (Shi et al., 2008; Nazer et al., 2016), large amounts of it are still stored in the environment with no specific use.

Cost-effectiveness and rapid production are among the reasons why the roller compacted concrete (RCC) is used in the construction of hydraulic structures and pavements of various roads and highways. During the 1970s, RCC pavements replaced the conventional asphalt types due to their higher construction costs (ACI 325.10R-95, 2001). Compared to the ordinary concrete: 1) RCC has less water content, more mineral additives (e.g., fly ash), and different manufacturing/execution processes (Wang et al., 2018), and 2) about 70–80% of its volume is composed of aggregates letting more voids to be filled with fine aggregates (ACI 325.10R-95, 2001). As RCC is spread with bulldozer in horizontal layers and is compacted by vibrating rollers (Liu et al., 2015), its post-curing behavior depends on how accurately and qualitatively the layers are implemented, compacted and controlled. Various parameters that should be considered to achieve an ideal RCC density include the speed and frequency of the roller vibration, number of its passes and the compressed thickness (NEAPRC, 2009). Compared to asphalt pavements, the RCC strength and durability are higher and show better performance against such oily elements as gasoline, diesel and grease (Rao et al., 2016), and compared to conventional concrete/embankment dams, construction of RCC dams is faster and more cost-effective, and involves material savings and less spillway cost due to smaller size and dimensions (Karimpour, 2010).

The industry growth and construction progress around the world

* Corresponding author. Civil Engineering Department, University of Sistan and Baluchestan, P.O. Box 98155 - 987, Zahedan, Iran.
E-mail addresses: ehsan_sheikh68@yahoo.com (E. Sheikh), s.r.mousavi@eng.usb.ac.ir (S.R. Mousavi), iman.afshun@gmail.com (I. Afshoon).

https://doi.org/10.1016/j.jclepro.2022.133005
Received 3 December 2021; Received in revised form 17 June 2022; Accepted 1 July 2022
Available online 16 July 2022

have boosted the need for large volumes of natural aggregates leading to the disposal of the related wastes and by-products and, hence, to potential environmental damage (Prem et al., 2018). Reducing the volume of waste materials and improving their recycling conditions are important issues in the waste and environmental management because natural resources are preserved and the required disposal space is reduced (Sharifi et al., 2015). About 3.7 billion tons of various aggregate types are used annually in the world (Association, 2018), and their production and consumption are still highly increasing compared to the past due to the concrete performance and special properties, and the increasing need of the related industries. As the concrete industry highly depends on natural resources for natural sand, much effort has been made in recent decades in many researches to reduce this dependence (Dhar et al., 2018). Introducing materials to replace natural aggregates can help limit the potential environmental damage and hazards due to the frequent use of natural resources (Mousavi et al., 2021). Therefore, approved, technical, economic waste collecting and disposing solutions can help keep the environment clean. The construction industry depends on the production of different-type/-quality concretes causing the annual consumption rate of which to be about 25×10^9 tons (IEA and WBCSD, 2009). Almost 55–80% of the concrete volume consists of aggregates most of which are produced either from riverbeds or by crushing mountain boulders that damage the environment seriously (Al-Jabri et al., 2009a). Only in 2015, aggregates used in the concrete industry amounted to about 48.3×10^9 tons (Freedonia, 2012). The need for large volumes of natural aggregates, mass production of industrial by-products/wastes and the related environmental degradation make it a task to see if it is possible to use various waste materials such as the CS as a substitute for natural aggregates in concrete. Certainly, the construction industry can, by the use of waste materials, proceed successfully and hopefully in future (Ambily et al., 2015). Replacing natural fine aggregates with the copper slag waste in concrete has economic, environmental, and practical benefits because the energy consumption and CO2 emissions are reduced, destruction of natural resources, due to their high consumption, is prevented and green, clean concretes are produced.

Outstanding features of the CS and its use in cement and concrete industries, especially in areas where it is in abundance, can have many environmental and economic merits (Shi et al., 2008). The use of copper slag powder as a cement substitute and its effects on the properties of different types of concrete have been investigated in different researches [freshness (Afshoon and Sharifi, 2014); durability (Najimi et al., 2011; Sharifi et al., 2020a,b); mechanical properties (Mobasher et al., 1996; Afshoon and Sharifi., 2017; Mirhosseini et al., 2017); thermal properties (Afshoon and Sharifi, 2020); fracture (Arino, and Mobasher, 1999)].

Al-Jabri et al. (2011) claimed that replacing 50% of the natural fine aggregates of cement mortars with the CS will increase the compressive strength by about 70%. Al-Jabri et al. (2009b) reported that when fine copper slag aggregates were used in high-performance concretes (0–100%), the density increased slightly (<5%), but the flowability increased considerably. According to them, up to 50% replacement improved the mechanical parameters, but above that (80–100%) reduced the compressive strength by 16%. Sharma and Khan (2017a) reported that increasing fine copper slag aggregates (0–60%) in the SCC increased the compressive and tensile strengths compared with those of the control mix design. They believed that about 20% replacement was the best to achieve the highest compressive strength and showed, by microstructural studies, that increasing the CS volume increased the pores, micro-cracks and capillary channels. Al-Jabri et al. (2009a) observed that while increasing the volume of copper slag aggregates improved the strength and durability of the high strength concrete (HSC), the water demand was reduced by about 22% at 100% replacement.

Wu et al. (2010a) believed that the improved flowability, efficiency and dynamic behavior of high strength concretes containing fine copper slag aggregates were related to the latter's smooth, polished surfaces and their less water absorption. They attributed the compressive, tensile and flexural strength drop of these concretes at more than 40% FeO_2 to the presence of excess water and higher CS fineness that caused micro-cracks and cavities to develop in the concrete microstructure. Wu et al. (2010b) reported that the desirable performance of concretes containing up to 40% fine copper slag aggregates under dynamic compressive strength was due to their improved mechanical properties. Achudhan and Vandhana (2018) observed that the compressive strength of RC beams improved by about 8.2% at maximum 40% CS replacement for natural fine aggregates. Sharma and Khan (2018) stated that using 100% fine copper slag aggregates and 10% metakaolin in the SCC not only increased its compressive and tensile strengths, but also reduced the carbonation depth, surface water absorption and sorptivity to achieve the desired quality (based on the UPV test). They recommend the use of such concretes in constructing tall buildings, bridge piers, in-situ and prefabricated piles, shallow and deep foundations and gravity dams. Examining the microstructure of SCCs containing fine copper slag aggregates, Gupta and Siddique (2019) concluded that the strength drop occurred above 30% replacement; formation of ettringite at 40% replacement and presence of pores and micro-cracks at 50 and 60% were other reasons for the strength drop. Vijayaraghavan et al. (2017) confirmed the significant improvement in the strength and mechanical properties of concretes containing 40% CS, 40% iron slag and 10% recycled concrete aggregates. After examining the properties of SCCs containing 0–100% fine copper slag aggregates, micro-silica and fly ash, Sharma and Khan (2017b) concluded that the compressive and tensile strengths increased in a 20–60% range of CS replacement. Using the scanning electron microscope (SEM) and energy dispersive spectroscopy (EDS), they examined the microstructure of specimens containing CS and confirmed the production of C–S–H compact gel after 120 days with a Ca/Si in the 0.77–1.11 range. Ambily et al. (2015) reported a 15–20% drop in the compressive strength of high-performance concretes (HPC) containing 100% fine copper slag aggregates, but believed that their use in producing these types of concretes was still cost-effective. Previous studies have reported improvements in the energy absorption, flexural capacity and fracture toughness parameters of flexural concrete beams containing fine copper slag aggregates (Prem et al., 2018). According to Khanzadi and Behnood (2009), coarse copper slag aggregates' suitable strength properties and strong bond could improve the strength properties of high strength concretes (HSC). Rezaei Lori et al. (2019) proposed a 60% CS replacement in the production of pervious concretes and believed that the results of the pull-off adhesion test resembled those of the slag-free concretes. According to their report, increasing the CS in such concretes increased their porosity and permeability. Sharifi et al. (2020a,b) reduced the W/C in SCCs containing coarse copper slag aggregates and improved the mechanical properties up to 100% replacement; the concrete production cost reduced by about 19% at full replacement. Gupta and Siddique (2020) claimed that the effects of using fine copper slag aggregates on the chlorine ion permeability were more evident at higher curing ages (90 and 365 days) and believed that the surface water absorption and capillarity reduced considerably in concretes containing less than 40% CS compared to the control mix design.

Examining 15, 30, 45, 60, 90 and 120 min RCC mixing-compaction times, Gharavi (2003) observed that increasing the delay time in relation to the optimized compaction time highly reduced the mix strength. Modarres and Hosseini (2014) studied the mechanical properties of RCCs containing recycled asphalt and rice husk ash (RHA) and claimed that the asphalt waste had negative effects on the mentioned properties and replacing cement with RHA by up to 5% reduced the rate of the strength drop. Fakhri and Saberi (2016) believed that using such cement additives as micro-silica by about 10% improved the RCC strength by about 20% while using only rubber wastes reduced it. Ali Ahmad et al. (2017) claimed that when the optimum moisture content was used to produce RCCs containing Lumachelle, the obtained strength was close to that of the concrete containing natural fine aggregates. Rooholamini

et al. (2019) reported that increasing fine-grained Electric Arc Furnace (EAF) steel slag reduced the mechanical parameters of the RCC, but increasing coarse grains improved the mechanical and fracture parameters significantly due to the desired angularity and roughness.

If these wastes are used as cement or natural aggregate substitutes in concrete elements aiming at producing clean, nature-friendly products, their collection from the environment will help the nature to face less damage for a period of time equal to the useful life-span of concrete structures. Even after the concrete element's life-span ends, it can be crushed, graded and reused as recycled waste materials in the production of fresh concretes; this cycle can probably be repeated many times.

This research addresses the environmental problems, concerns and consequences of leaving large copper-slag volumes in the nature. It tries to eliminate the related natural-aggregate-production damage to the nature by studying the feasibility of replacing CS for natural fine aggregates in the nature-friendly RCC and investigating its mechanical and microstructural characteristics. To this end, the RCC's natural fine aggregates were replaced with 0, 10, 20, 30, 40, 50 and 60% CS and results of the mechanical tests were validated scientifically using SEM images. To the authors' best knowledge, this is the first comprehensive research on using fine copper-slag aggregates in the RCC, and the results have confirmed that green, nature-friendly RCCs containing CS can be produced to solve their related environmental waste problems.

2. Experimental plan

This section addresses defining materials specifications, designing mix-design ratios, selecting dimensions, preparing specimens and performing tests.

2.1. Materials

Table 1 lists the characteristics of Type II cement (based on ASTM C 150–09, 2009) used to prepare the required RCC specimens, and Table 2 shows those of the natural fine and coarse aggregates (according to ASTM C 29M-09, 2009; ASTM C 127-07, 2007; ASTM C 128-07, 2007; ASTM C 1252 – 03, 2003). Fine aggregates, with maximum diameter = 4.75 mm, were collected from rivers and coarse aggregates, with maximum diameter = 19.5 mm, were prepared by crushing boulders available in Zahedan City, Iran; Fig. 1 shows the gradation of the natural aggregates (ASTM C 33M-08, 2008).

Large copper-slag volumes, first introduced as by-products and wastes in biological refining processes to produce pure copper, need stockpiling, recycling and metal recovery methods for their management (Ong, 2009). When producing pure copper, the related slag wastes are molten-separated and then cooled by either water or air. In the former, aggregates have an amorphous structure, high porosity, lower specific gravity and greater absorbability, but in the latter, they have dense, stiff structures and desirable mechanical properties such as excellent soundness, desirable abrasion resistance and good stability to replace natural aggregates (Gorai et al., 2003; Mirhosseini et al., 2017). The CS used in this research is black, angular and broken, and has smooth surface and rough texture (Figs. 2–4). According to Fig. 4, the consumed CS has a crystalline structure and lacks reactivity. It has been prepared from the melting factory of Sarcheshmeh mineral complex, Iran, with an annual production rate of about 360,000 tons (Mirhosseini et al., 2017). This study has used the air-cooled CS to replace natural fine aggregates due to its suitable structure and good physical characteristics. Physical and chemical properties of this material are shown in Tables 2 and 3, respectively. It consists of copper compounds (0.7%), alumina (4–5%), calcium oxide (4–6%), silica (30–34%) and iron (35–37%) (Afshoon and Sharifi, 2017) and, compared to natural aggregates, it is heavier (G = 3.15 g/cm^3) and absorbs less water (0.2%). To prepare and cure the specimens, use was made of the urban drinking water (ASTM C 94M-09, 2009).

Table 1
Properties of type II Portland cement of Sistan Cement Factory.

Chemical properties (%)	Results	Physical properties	Results
SiO_2	21.47 ± 0.28	Specific surface area (cm^2/g)	3110
Al_2O_3	5.40 ± 0.11	Setting time (initial) (min)	183
Fe_2O_3	3.82 ± 0.14	Setting time (final) (min)	238
CaO	62.52 ± 0.32	Autoclave Expansion (%)	0.08
MgO	1.31 ± 0.24	Compressive strength (3 Days) (MPa)	26
Na_2O	0.65 ± .0.05	Compressive strength (7 Days) (MPa)	34
K_2O	0.43 ± 0.03	Compressive strength (28 Days) (MPa)	44

Table 2
Characteristics of used natural aggregates and CS.

Component	Properties		
	Specific gravity	Void content (%)	Water absorption (%)
Fine aggregate	2.73	36.71	1.09
Coarse aggregate	2.81	47.58	0.32
CS aggregate	3.53	—	0.2

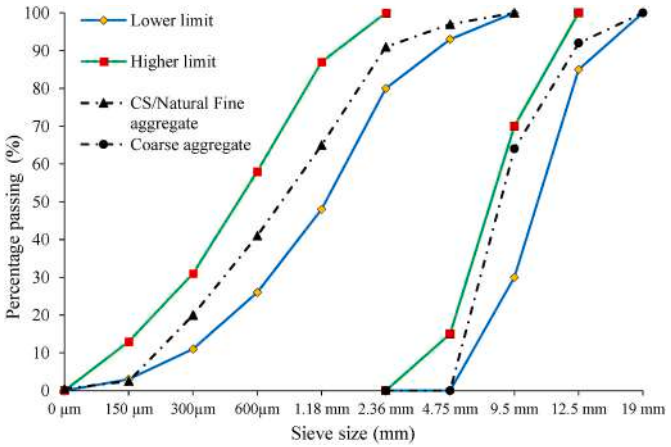

Fig. 1. Particle size distribution of CS/natural fine and coarse aggregates.

2.2. Mix design proportions

In this research, RCC mix-design proportions are based on the Iranian regulations (Iranian code 354, 2009), and natural fine aggregates have been replaced with 0 (Control), 10, 20, 30, 40, 50 and 60% fine copper slag aggregates named RCC0 (Control), RCC10, RCC20, RCC30, RCC40, RCC50 and RCC60, respectively. As regulations suggest 12–16% cement, by total weight of aggregates, to produce RCCs with optimal flexural strength, this study used a value of 14% (284 kg/m^3). Considering the maximum aggregate size (19.5 mm) and values required by the Iranian regulations, natural coarse aggregates ranged from 48 to 52% of the total concrete volume; hence, fine and coarse aggregates amounted, respectively, to 48 and 52% in all mix designs to produce RCCs with/-without CS. A fix value of W/C = 0.38% was considered for all RCCs because of its direct effects on the concrete strength; specifications and details of all mix designs are listed in Table 4.

2.3. Preparing specimens

Before mixing the materials, the molds were cleaned and lubricated to prevent the specimens from breaking and chipping when molds

Fig. 2. Copper slag used in this study: A) Coarse aggregates (crushed large pieces), B) Fine CS aggregates, C) Gradation of fine CS aggregates.

opened. Materials, with known weights, were poured and mixed in a rotary planetary mixer and the fresh concrete, prepared based on ASTM C 1435 – 08 (2008), was poured in three layers each of which was fully compacted by a vibrating hammer for 20 s. Surfaces of the molds were smoothed with a ruler and a steel plate and then covered with plastic sheets for 24 h to prevent evaporation and moisture loss. Finally, the molds were carefully opened after 24 h and the specimens were

Fig. 3. SEM morphology of copper slag.

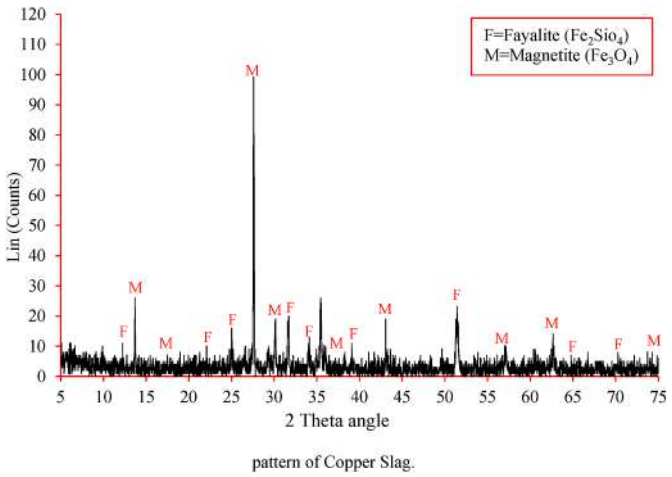

Fig. 4. XRD pattern of Copper Slag.

transferred to a 23 °C water tank for curing.

2.4. Testing the specimens

Compressive and tensile strengths were the averages found for three 150 × 300 mm cylindrical specimens cured for 7, 28 and 91 days (ASTM C 39M – 09, 2009; ASTM C 496M-04, 2004), the flexural strength was the average found for three 100 × 100 × 400 mm beams (same curing periods) (ASTM C 78-09, 2009; ASTM C 1690M-12, 2012) and the water absorption of the RCC containing fine copper slag aggregates was the average of three 100 × 100 × 100 mm cubic specimens (ASTM C 642-06, 2006) (Eq. (1) below). After 28 days curing, the specimens required for water absorption tests were kept in an oven for 24 h at a temperature of about 105 °C to gain a constant weight (less than 5% difference between two measured weighs), their dry weights were recorded and they were then placed in a water tank to determine their saturated weights. Next, they were cleaned well with a piece of linen cloth and their saturated weights were measured after 1 h and 3, 7, 28 and 91 days.

$$Water\ absorption = \frac{W_S - W_D}{W_D} \quad (1)$$

Capillarity, too, was calculated using the mentioned cubic specimens. To isolate them, their four sides were covered with paraffin wax and their dry weights were recorded. Their top and bottom sides were uncovered so that water could move from bottom to top. Using Hall's method (1989), the sorptivity coefficient was calculated at 0.5, 1, 5 and 24 h time periods as follows:

$$K = \frac{Q^2}{A^2 T} \quad (2)$$

where K, Q, A, and T are the sorptivity coefficient ($cm/s^{0.5}$), adsorbed water (cm^3), section area (cm^2) and time (s), respectively.

To calculate the water penetration depth, three 150 × 300 mm 28-day cylindrical specimens (BS EN12390-8, 2000) were subjected to constant water pressure for about 72 h and the mentioned depth was measured after they failed. As the concrete specific gravity depends on the aggregate density, and replacing cement with other materials does not change it much, specific gravity measurements were done on 28-day RCC specimens containing different CS percentages (BS EN 12390, 2009).

This research presents images of some inner parts of fractured specimens with major changes in their morphologies provided by SEM-based microstructural analyses. Fig. 5 shows the cross section of the RCC20, RCC40 and RCC60 specimens.

3. Results and discussion

To evaluate the performance and behavior of various concrete types, it is necessary to perform strength tests (compressive, tensile and flexural) and review and analyze the related results. Studying other characteristics (surface and capillary water absorption, water penetration, and unit weight) and investigating the microstructural and economic aspects will also provide the consumer with a better understanding of the performance and application of the produced concrete. This section has studied the properties of RCCs with/without CS using the results of various tests.

3.1. Compressive strength

The compressive strength test results of 7-, 28- and 91-day specimens with/without CS are shown in Fig. 6; as shown, the strength of concretes containing fine copper slag aggregates (at all ages) is equal to/greater than that of the control specimen and lies in the 24.23–27.10, 27.69–32.40 and 31.64–39.11 MPa ranges, respectively. At all ages, RCC40 has the highest compressive strength being more by 11.84, 17.01 and 23.58% than that of the mix-design containing 100% natural sand for, respectively, 7-, 28- and 91-day specimens. SEM-image morphology studies of copper slag-free SCC show that the 28-day cement-paste matrix structure contains numerous unhydrated particles, cavities and ettringite pieces (Fig. 7A). These factors cause RCC0 to show less resistant compared to designs containing CS. As increasing the age from 28 to 91 days improves the hydration process over time, unhydrated particles and ettringite pieces become smaller causing the strength to increase (Fig. 7B). But, Fig. 7C–F shows that ettringite pieces are

Table 3
Characteristics of Copper slag (Sharifi et al. (2020a,b)).

Component (%)	SiO_2	Al_2O_3	Fe_2O_3	CaO	MgO	Na_2O	K_2O	Cu	SO_3	LOI
Results	34	2	48.78	4.89	1.23	0.63	2.37	0.43	3.26	1.65

Table 4
RCC mixtures properties.

Component (Kg/m3)	RCC0	RCC10	RCC20	RCC30	RCC40	RCC50	RCC60
Cement	284	284	284	284	284	284	284
Water	108	108	108	108	108	108	108
Natural fine aggregate	973	876	778	681	584	487	389
Fine copper slag aggregate	0	97	195	292	389	487	584
Natural coarse aggregate	1055	1055	1055	1055	1055	1055	1055
Water/Cement (%)	0.38	0.38	0.38	0.38	0.38	0.38	0.38
Natural Fine agg./Total agg. Ratio	0.48	0.45	0.42	0.39	0.36	0.32	0.27
Natural Coarse agg./Total agg. Ratio	0.52	0.52	0.52	0.52	0.52	0.52	0.52

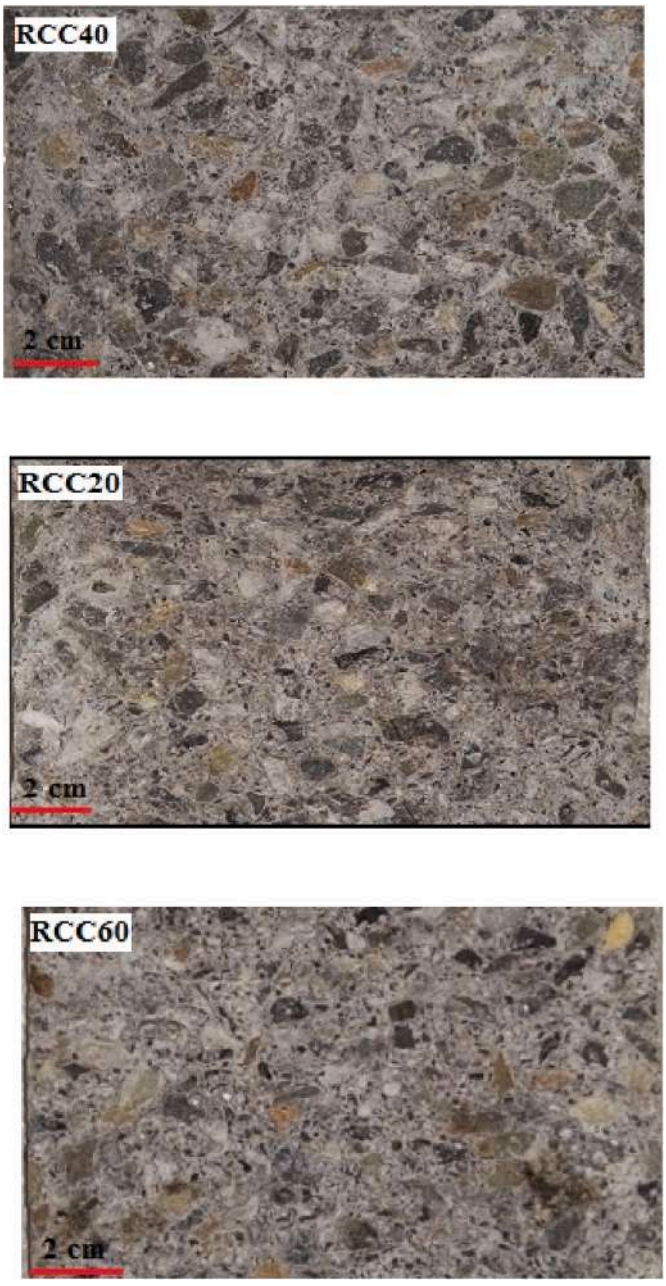

Fig. 5. The cross-sectional view of RCC20, RCC40 and RCC60.

removed from the morphology of RCC20 and RCC40 at the ages of 28 and 91 days and the size of pores and unhydrated particles are highly reduced. Dense C–S–H structures in RCC20 and RCC40 have highly improved the strength, especially at 91 days. Improved strength properties of RCC20 and RCC40 can be due to the special balance established between the free water not absorbed by the CS and that required to complete the hydration process. In high-copper-slag concretes (28 days), cracks, unhydrated particles and cavities cause the strength to decrease compared to RCC20 and RCC40 (Fig. 7G). In (Fig. 7H), the RCC60 morphology shows smaller cavities and less unhydrated particles. The SEM-image comparison of RCC0 and RCC60 shows that the latter has a more integrated and uniform C–S–H structure and is stronger than RCC0 because its ettringite pieces are removed. It is worth noting that the pozzolanic activity of the CS used in this study is quite low and the filling impact of these waste materials is an important factor that improves the concrete strength and creates a denser microstructure; meanwhile, we should not forget the high stiffness and strength of CS grains that play an

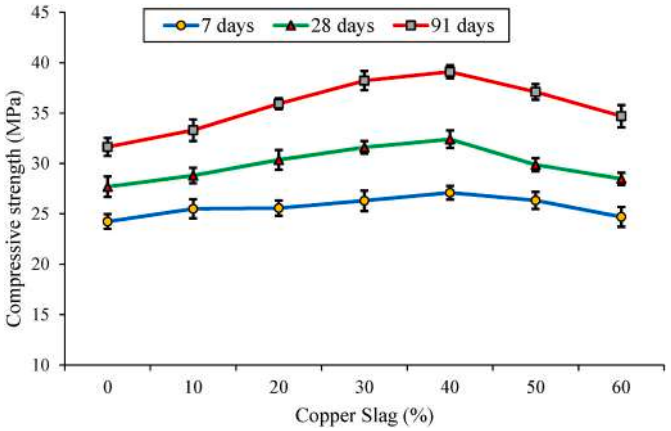

Fig. 6. The results of compressive strength of RCCs.

important role in increasing the concrete compressive strength. For the 7–day specimen, the RCC60 strength drop is because heavy metals in the copper slag aggregates delay the setting and hydration processes (Sharma and Khan, 2017a). According to Gupta and Siddique (2020), the compressive strength of SCCs containing CS increases up to 30% replacement, and the increase rate is more from 7 to 28 days. This phenomenon is attributed to the physical features, corner sharpness and angularity of copper slag aggregates that cause better locking with the cement paste (Al-Jabri et al., 2011; Gupta and Siddique, 2019). Higher density and compressibility of copper slag aggregates compared to natural fine aggregates have positive effects on the stress concentration of the paste and concrete components (Wu et al., 2010a). Despite the strength drop above 40% replacements, RCC60 showed an increase of 1.94, 2.85 and 9.67% increase at ages of, respectively, 7, 28 and 91 days (Gupta and Siddique, 2020). In high copper-slag specimens, the strength drop is due to the smooth glassy surface texture and low water absorption of the copper slag aggregates that cause the excess water to remain in the concrete (Khanzadi and Behnood, 2009; Sharma and Khan, 2017a).

As the interfacial transition zone (ITZ) is the weakest link in the concrete matrix, its characteristics should be checked and controlled well (Sharma and Khan, 2017a). Microstructural studies of RCCs containing high volumes of CS (50–60%) show that the strength is reduced due to the deposition of copper slag aggregates that are heavier than natural ones. Because of this phenomenon, the excess water moves up towards the surface of the fresh concrete and causes porous microstructure, more micro-cracks, continuous capillary voids, cracks in the ITZ and increased thickness of this area (Fig. 8I-L).

Table 5 lists the ratios of different-age compressive strengths of all specimens to that of the 28-day control design; as shown, 7-day CS specimens were able to achieve more than 0.89 of the strength of the 28-day control design concluding that they can be used in applications that require premature strength. The 91-day compressive strengths of RCC10, RCC20, RCC30, RCC40, RCC50 and RCC60 are, respectively, 1.14, 1.20, 1.30, 1.38, 1.41, 1.34 and 1.25 times that of the 28-day RCC0. Since compressive strength is the most important feature of concrete, pavement designers can confidently use CS in RCC pavements because it has desirable strength at different ages.

3.2. Split tensile strength

Fig. 9 shows the split tensile strength of RCCs containing 0–60% CS; as shown, an increase in percent copper slag replacement increases the tensile strength at all ages. At high replacements, the tensile strength growth rate of the 7-day specimen is more uniform and lies in the range of 2.23–2.65, 2.84–3.35 and 3.13–3.59 MPa for, respectively, 7-, 28- and 91-day specimens for all mix designs. The RCC60 tensile strength shows

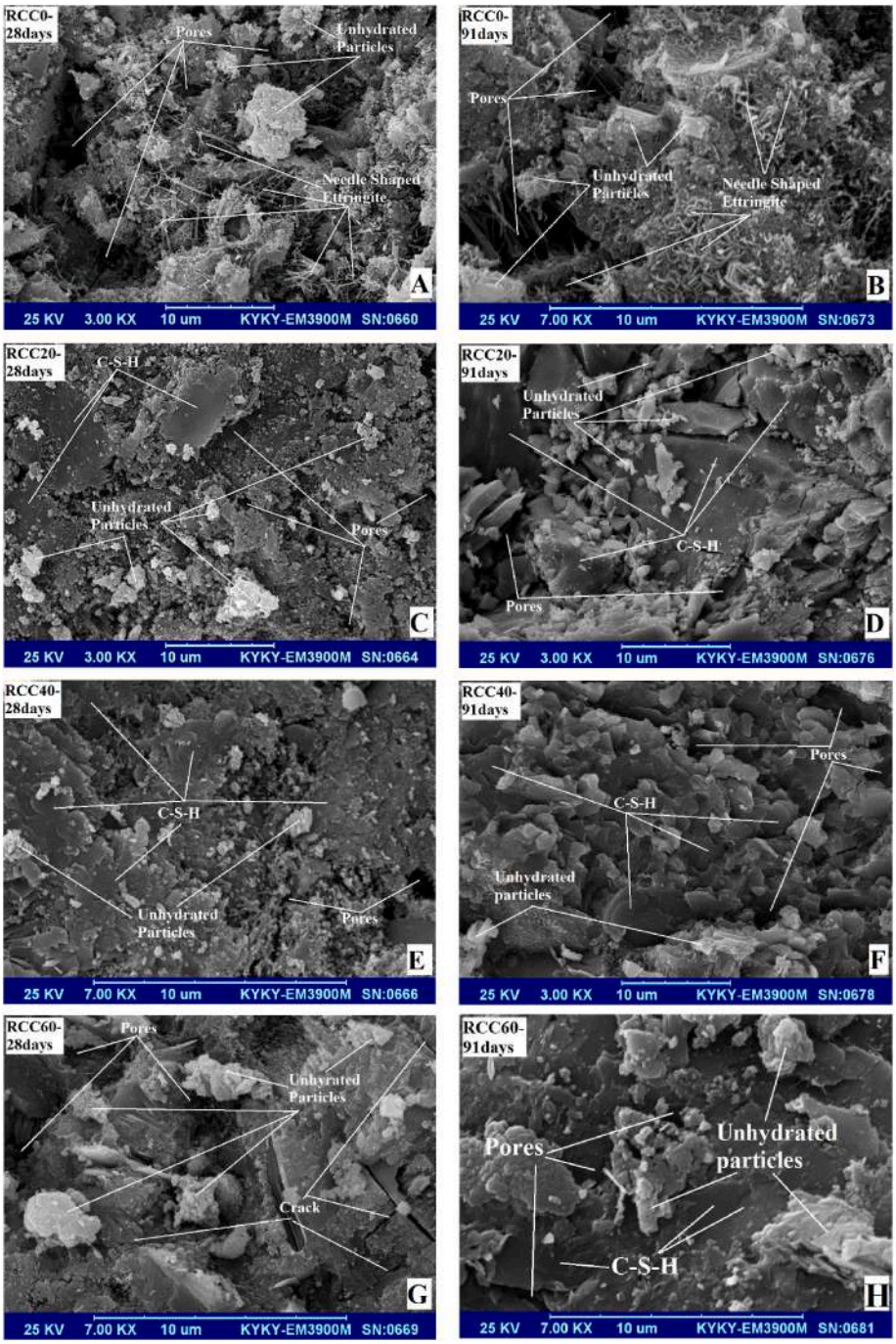

Fig. 7. SEM images of RCCs at different curing times: A) RCC0-28 day B) RCC0-91 day C) RCC20-28days D) RCC20-91 day E) RCC40-28 day F) RCC40-91 day G) RCC60-28 day H) RCC60-91days.

18.83, 17.96 and 14.70% increase in the mentioned specimens compared to RCC0, and 26.42 and 35.47% increase in, respectively, 28- and 91-day specimens compared to the 7–day specimen. Gupta and Siddique (2019) reported an increase in the RCC tensile strength at up to 60% CS replacements and Sharma and Khan (2017a) reported the same increase in the 0–80% replacement range. Al-Jabri et al. (2009a) observed a 19% increase in the tensile strength of high-strength concretes containing 100% CS compared to the control design and Rezaei Lori et al. (2019) confirmed the tensile strength increase of the mentioned concretes containing 0–60% coarse CS aggregates. It is believed that the tensile strength increase of CS specimens is due to the angularity and stronger CS aggregate bond with the cement paste (Khanzadi and Behnood, 2009; Sharma and Khan, 2017a).

According to (Fig. 7A–B), abundance of cavities - sometimes with large dimensions - in the RCC0 morphology, and non-formation of a dense, suitable C–S–H structure cause cracks to propagate and expand quickly and easily when the copper slag-free concrete is subjected to tensile stress. In fact, when the crack tip reaches the cavity space, not only will the crack propagate and expand quickly, but it will also deflect, especially towards weaker areas; here, the tensile strength will sharply drop due to the speed in the crack development process. But when 20 and 40% copper slag replace natural aggregates (Fig. 7C–F), they not only improve the concrete properties due to their good stiffness, sharpness and better adhesion to the cement paste, but also enhance the hydration process (for using the free water), improve the cohesion of the C–S–H structure, reduce dimension of cavities, omit micro-cracks (as a

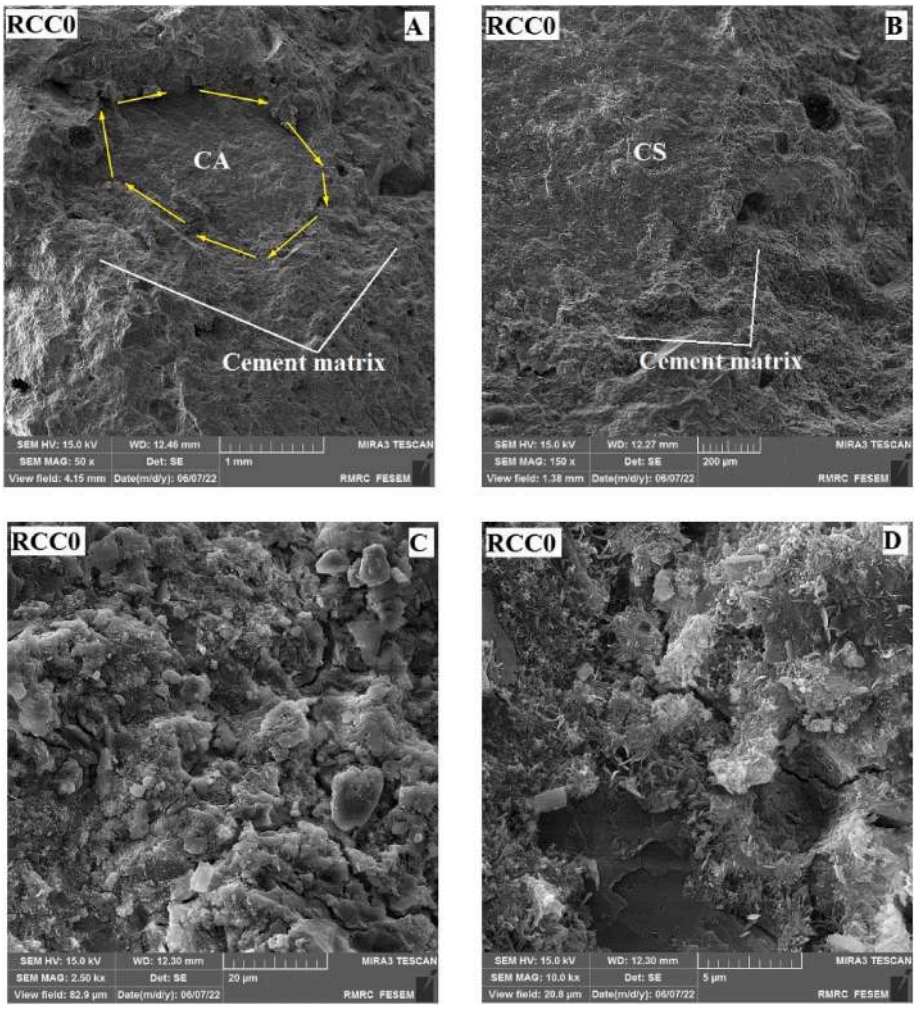

Fig. 8. SEM images of ITZ: A-D) RCC0 E-H) RCC40 I-L) RCC60.

barrier against crack growth) and, hence, improve the tensile strength. Although SEM images confirm cavities in the RCC60 morphology (Fig. 7G–H), increasing the CS in concrete has caused the positive effects of the physical properties of this waste material to be more compared to the negative effects of the free water (creating cavities and microcracks); growth of the tensile strength is still visible.

Increased strength and improved ITZ create brittle behavior in concrete because the crack path will pass through aggregates and reduce the bond (Beygi et al., 2014). SEM images show that in low CS concretes, an increase in water will improve the paste-matrix microstructure and compresses the ITZ because CS aggregates absorb less water. On the other hand, the high CS aggregate stiffness does not allow cracks to pass through them causing the tensile strength to increase, but when the CS volume increases in the concrete, the increased W/C causes porosity and capillary voids in the ITZ. Although voids and porosity are created in the ITZ of high CS concretes, the aggregate angularity of this waste material will lead to better interlocking with the cement paste, longer crack path, obstacles in the crack propagation, reduced void effects in the ITZ and, hence, improved tensile strength (Fig. 8E).

Table 6 shows the tensile strength ratios of different-age specimens with/without CS to that of the 28-day control design. The 7-, 28- and 91-day RCC60 specimens achieved tensile strengths of, respectively, 0.94, 1.18 and 1.26 times that of the 28-day specimen containing natural aggregates. The 28-day RCC10 had a tensile strength slightly more than that of the RCC0.

3.3. Flexural strength

Fig. 10 shows the flexural strength variations of the 7-, 28- and 91-day CS RCC specimens; as shown, at all curing ages, the flexural strength increases with an increase in the CS compared to the control specimen and lies, respectively, in the range of 3.56–4.42, 3.86–4.72 and 4.33–5.15 MPa for all concretes with/without CS. RCC60 shows 22.19, 22.28 and 18.94% increase for the mentioned ages compared to RCC0 and a slight decrease compared to RCC50 for the 7-day specimen. While Al-Jabri et al. (2009a) reported flexural strength improvements of up to 50% for concretes containing coarse CS aggregates, Sharifi et al. (2020a,b) attributed this increase to the dense structure of CS aggregates and their good bond with the cement paste. According to Prem et al. (2018), full CS replacement for natural fine aggregates is quite possible in flexural members due to the appropriate structural behavior of this type of concrete. The flexural strength drop of high CS concretes is attributed to the increased free water and, thus, formation of more pores in the concrete structure (Wu et al., 2010a).

Table 7 shows that only RCC10 and RCC20 have reached about 0.92 and 0.96% strength of the 28-day control design, but 7-day concretes containing 20–60% CS were able to achieve strengths greater than that of the 28-day, CS-free concrete. Concretes with this feature can be used in flexural elements that either undergo short-time loading or need quick stripping to increase the construction speed. The flexural strength of the RCC60 increases by about 13, 22 and 33% for, respectively, 7-, 28 and 91-day specimens compared to the 28-day CS-free concrete.

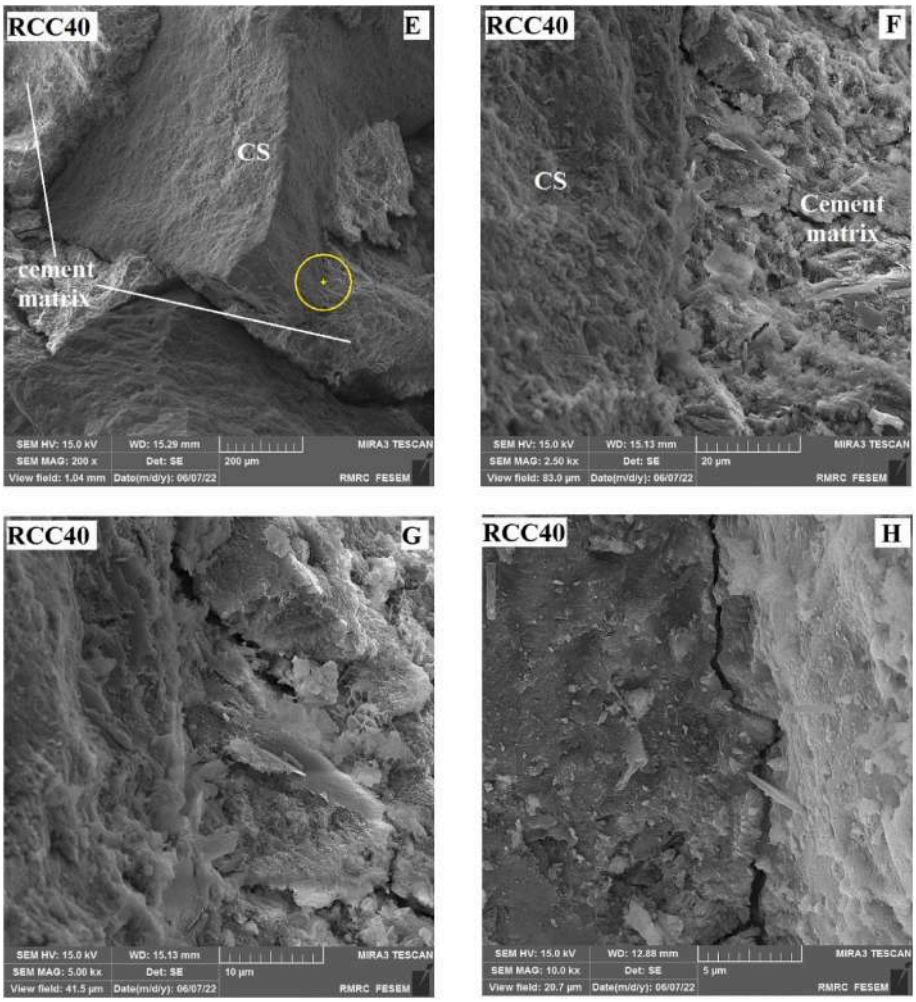

Fig. 8. (*continued*).

3.4. Surface water absorption

Studying surface water absorption of different concrete types can lead to a better understanding of the performance and behavior of their freeze-thaw cycles (Sharifi et al., 2016). Fig. 11 shows this absorption for different-age specimens containing 0, 10, 20, 30, 40, 50 and 60% CS; as shown, increasing the CS reduces the absorption compared to the control specimen; RCC40 has the lowest absorption rate among all specimens except the RCC30 for which the rate is the lowest at 1 h age. The 1 h and 1-, 7-, 28- and 91-day age RCC60 absorption rate reduced by, respectively, 5.31, 6.49, 18.20, 19.63 and 20.34% compared to the RCC0 indicating that the older is the specimen, the more effective is the CS participation in chemical hydration reactions and more pores become blocked. RCC40's reduced surface absorption compared to different-age RCC0s is in the 23.68–33.35% range. The absorption rate of all 91-day specimens is less than 7% increasing by, respectively, 84.64, 72.17, 63.89, 55.71, 36.09, 44.37 and 47.19% compared to the 1 h specimen if the CS increased from 0 to 60%. In fact, large cavities in the RCC0 morphology will create a suitable storage for the absorbed water and increase the water absorption rate (Fig. 12A). On the other hand, ettringite pieces will create a porous space in the concrete structure, which causes water to transfer from one cavity to another (Fig. 12A). SEM images show that although RCC20 cavities are small in size, they are plenty and make a good place to store water (Fig. 12B). In RCC60, although cavities are not many, they are large in dimensions and absorb more water than RCC40 (Fig. 12C). According to SEM images, the hydration products and higher C–S–H gel volumes in concretes containing 10, 20, 30 and 40% CS have caused the concrete-matrix microstructure to be more consistent and uniform causing less water to penetrate from around the specimen, and the surface water absorption to be controlled properly. Sharma and Khan (2017b) believed that although the surface water absorption of specimens with more than 50% CS had an increasing trend, the produced concrete absorbed less water than the control design. While Prem et al. (2018) claimed that using fine CS aggregates in concrete reduced the surface water absorption, Sharifi et al. (2020a,b) reported that controlling the w/c and achieving optimal mechanical properties and durability in concretes containing 100% coarse CS aggregates reduced the surface water absorption by about 8.1% after 90 days curing.

3.5. Capillary water absorption (Sorptivity)

Sorptivity is the parameter used to study how unsaturated concretes behave under water penetration (ASTM C 1585-04, 2004). This parameter is mostly affected by the mix proportion, aggregate characteristics, supplementary cementitious materials, additive type/amount and the concrete pouring method (Gesoglu et al., 2016). Fig. 13 shows the sorptivity test results of all RCCs containing 0–60% CS. As shown, the trend is generally reducing for all designs when the CS increases; a 0–40% increase reduces the absorption although there is a slight increase in RCC50 and RCC60, but it is still less than that of the control design. 24 h after testing, this parameter showed a reduction of 19.21, 34.23, 49.61, 79.46, 62.79 and 56.20% for, respectively, RCC10, RCC20, RCC30, RCC40, RCC50 and RCC60 compared to the RCC0. RCC0

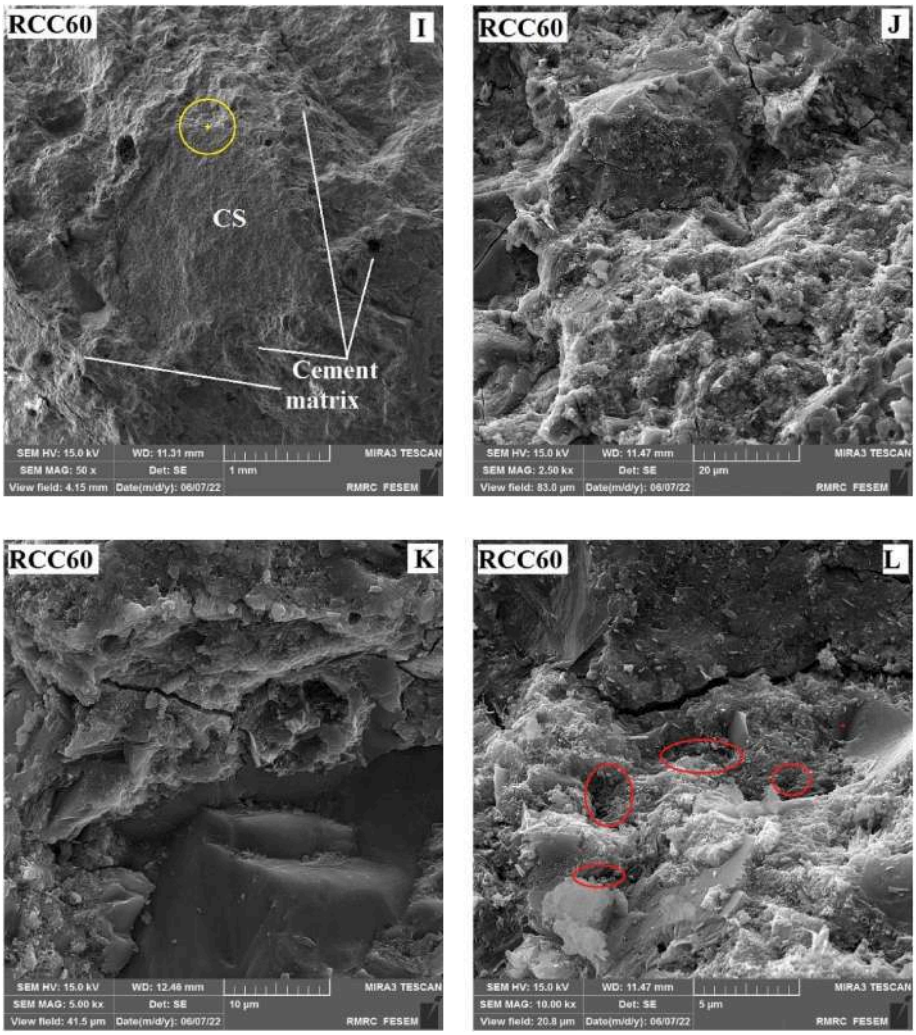

Fig. 8. (*continued*).

Table 5
Relative compressive strength (F_c/F_{c28}).

Age	RCC0	RCC10	RCC20	RCC30	RCC40	RCC50	RCC60
7 days	0.88	0.92	0.92	0.95	0.98	0.95	0.89
28 days	1.00	1.04	1.10	1.14	1.17	1.08	1.03
90 days	1.14	1.20	1.30	1.38	1.41	1.34	1.25

Table 6
Relative split strength (F_t/F_{t28}).

Age	RCC0	RCC10	RCC20	RCC30	RCC40	RCC50	RCC60
7 days	0.79	0.81	0.86	0.88	0.91	0.93	0.94
28 days	1.00	1.03	1.08	1.11	1.13	1.15	1.18
91 days	1.10	1.12	1.16	1.19	1.21	1.24	1.26

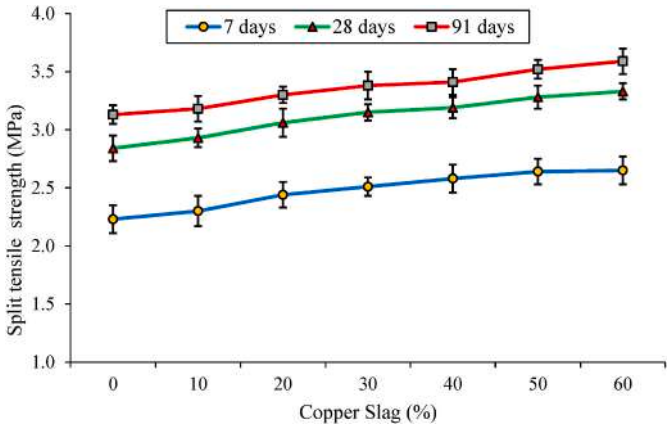

Fig. 9. The results of splitting tensile strength of RCCs.

microstructural studies confirm the presence of large continuous voids through which water easily passes and fills the empty spaces, but increasing the CS up to 40% creates a stiffer, better-quality microstructure in the concrete matrix that fills part of the voids and cuts the connection of the capillary voids. In high CS concretes, although voids are small and the crack length is short, the concrete microstructure has a lower quality and sorptivity is slightly increased.

Gupta and Siddique (2020) stated that: 1) concretes containing 30% fine CS aggregates had a lower initial sorptivity rate, which increased slightly at higher CS values, and 2) all CS mix designs had less sorptivity rates than the control design. Nematollahzade et al. (2020) claimed that reducing W/C reduced the sorptivity and concluded that the increasing trend in RCC50 and RCC60 was due to low CS aggregate absorption rate that increased the free water in concrete. Some researchers have reported a good correlation between the improved strength and reduced adsorption, and have claimed that reducing sorptivity would increase the compressive strength (Siad, 2010; Samimi et al., 2017). Siddique

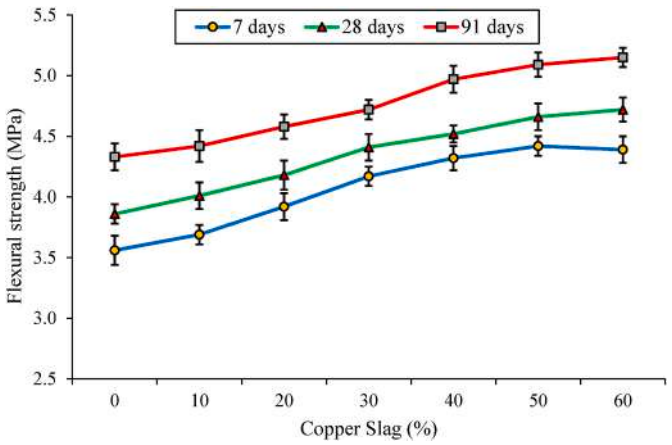

Fig. 10. The results of flexural tensile strength of RCCs.

Table 7
Relative flexural strength (F_r/F_{r28}).

Age	RCC0	RCC10	RCC20	RCC30	RCC40	RCC50	RCC60
7 days	0.92	0.96	1.02	1.08	1.12	1.15	1.13
28 days	1.00	1.04	1.08	1.13	1.17	1.21	1.22
91 days	1.12	1.15	1.19	1.22	1.29	1.31	1.33

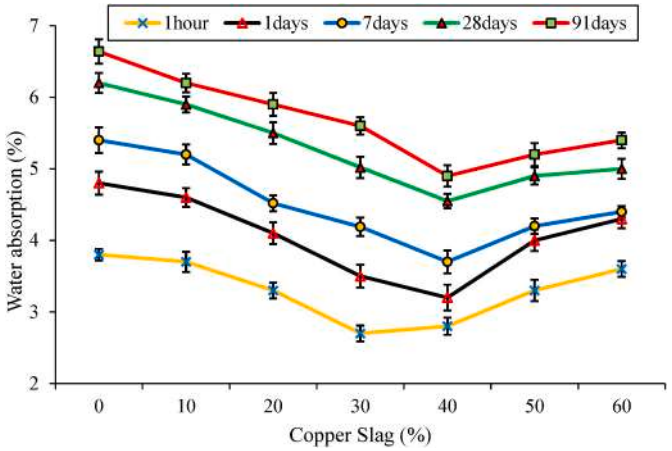

Fig. 11. The results of surface water absorption of RCCs.

et al. (2019) showed that: 1) improving the microstructure of the copper-slag steel fiber reinforced concretes (CSSFRC) reduced the internal voids and capillary channels, causing the total sorptivity to be reduced and 2) the CS content and sorptivity were related linearly and had a good correlation (R2 = 0.876). Sharma and Khan (2017c) showed that after 120 days curing, the sorptivity of RCC60 specimens was reduced. Rajasekar et al. (2019) introduced ultra-high strength RCC60s as highly impermeable concretes due to their low sorptivity.

3.6. Water penetration

Concrete permeability, due to channels and pores, provides conditions for chlorides and salts to attack the concrete structure and the water to pass through the pores and rust the rebars. Reduced voids in CS concretes are attributed to the increased aggregate packing (Obe et al., 2016). The water penetration depth can be used to investigate the superficial porosity and Fig. 14 shows this parameter for 28-day concretes with/without CS. All CS RCC specimens have less water penetration depth than RCC0; RCC40 has the lowest. The increase in the penetration

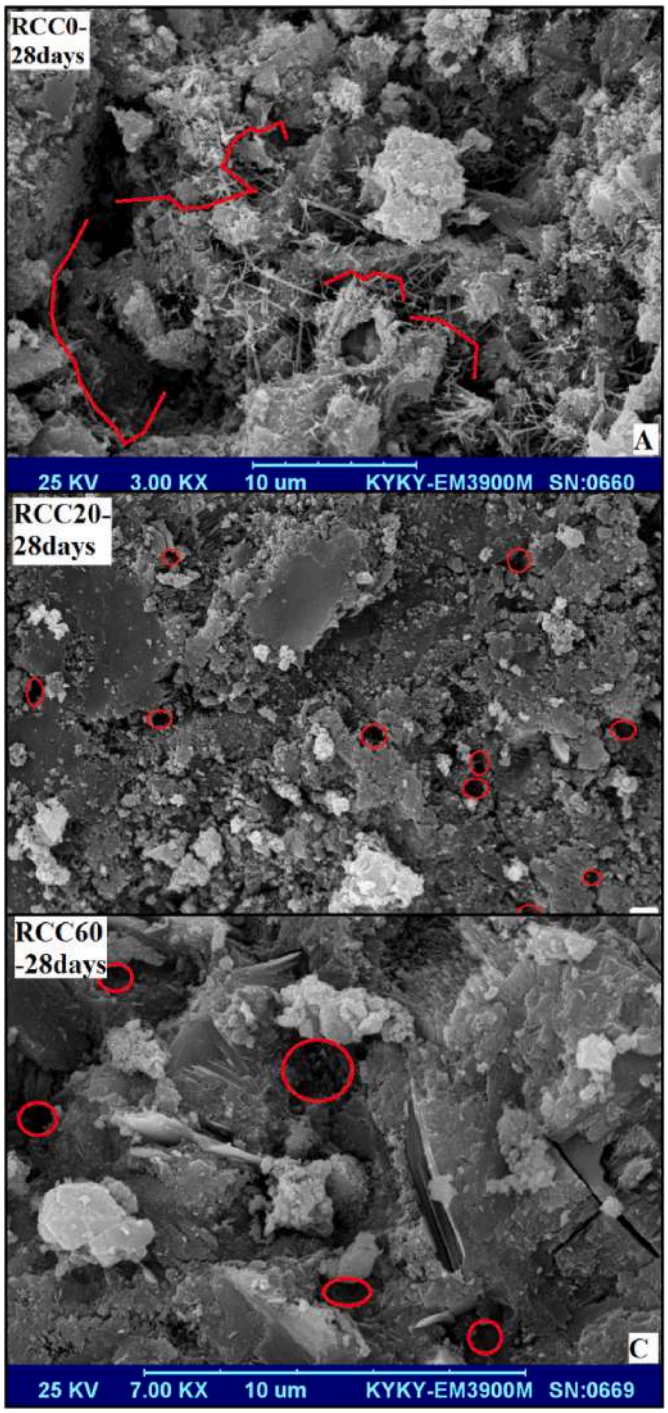

Fig. 12. Water transfer routes and storage sites of absorbed waters: A) RCC0 B) RCC20 C) RCC60.

depth is more in RCC50 and RCC60 than in RCC40, but compared to RCC0, they show 26.91 and 23.12% decrease, respectively. High C–S–H gel volume and reduced un-hydrated particles in the CS concrete microstructure has blocked the capillary voids and highly reduced the empty spaces in the concrete-matrix structure; this is why conditions for water to penetrate into the concrete structure are almost eliminated. Afshoon and Sharifi (2017) have attributed the decrease in the CS concrete water permeability to the formation of the C–S–H gel due to the reaction between the CS silica and the $Ca(OH)_2$. Siddique et al. (2019) believe that increasing the fine CS aggregates in SFRC will increase the hydration products, improve the concrete microstructure and reduce the

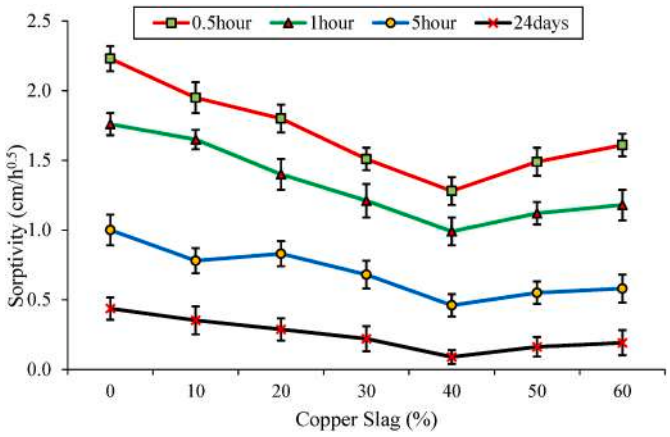

Fig. 13. The results of water absorption coefficient of RCCs.

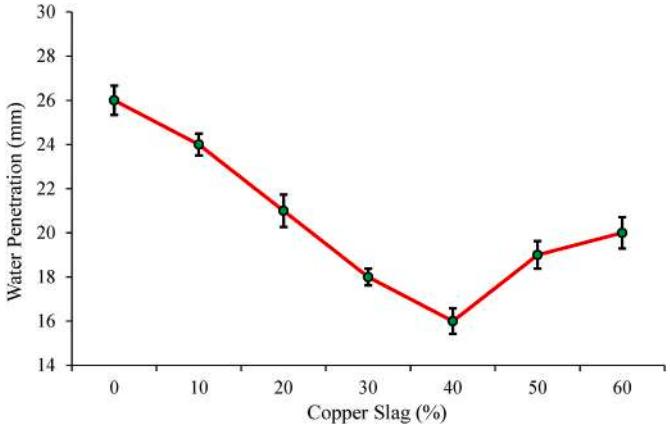

Fig. 14. The results of water penetration of RCCs.

aggregates' water absorption because capillary channels are disconnected, pores are reduced and permeability paths are blocked. Using CS in the SFRC (as a substitute for stone materials) will fill the internal pores and, hence, improve its behavior (Boakye and Uzoegbo, 2014).

3.7. Unit weight

Unit weight of RCCs containing different CS percentages is shown in Fig. 15; as shown, increasing the CS from 0 to 60% increases the unit weight from 2356 to 2550 kg/m^3. RCC10 to RCC60 show a unit weight

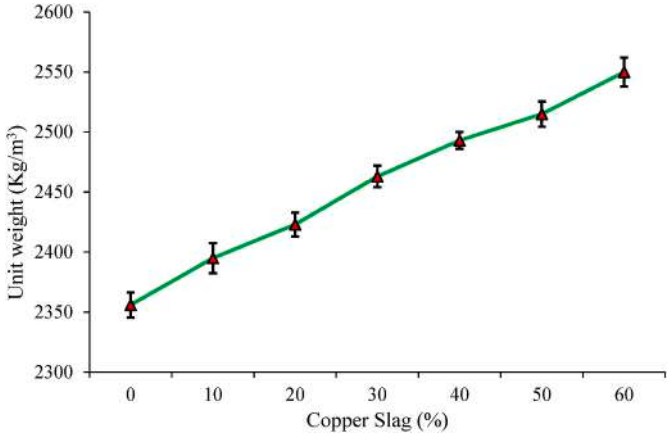

Fig. 15. The results of unit weight of RCCs.

increase of, respectively, 0.38, 1.55, 1.98, 4.48, 5.41 and 6.87% compared to RCC0 due to higher aggregate density compared to natural fine aggregates (Sharifi et al., 2020a,b). Replacing cement with the CS powder will cause a slight increase of about 2.5% in the concrete unit weight (Afshoon and Sharifi, 2017). Al-Jabri et al. (2009a) claimed that using CS as fine aggregates in high-strength concretes will increase the unit weight by 8%. Using 100% coarse CS aggregates in the SCC and pervious concrete will increase the unit weight by, respectively, 15 and 26% (Rezaei Lori et al., 2019; Sharifi et al., 2020a,b); this increase enables these concretes to be used in the construction of tunnels, pavements, gravity concretes, deep/shallow foundations, dams/hydraulic structures, bridges and piles (Sharma and Khan, 2018).

3.8. Microstructural analyses

Performance and behavior of the hardened concrete are directly affected by its microstructural quality which is influenced by such factors as the curing time, cement type, materials, hydration process quality, W/C and mineral additives (Singh and Siddique, 2016). To study the concrete microstructure, its matrix morphology and topography can be evaluated and analyzed using micrograph SEM images obtained by performing compressive strength tests on some isolated gold-coated fragments of the inner part of the fractured specimen. For a better comparison, SEM images of the 28- and 91-day RCC0, RCC20, RCC40 and RCC60 specimens are shown in Fig. 7. Fig. 7A shows that at the age of 28 days, large cavities, long ettringite pieces and much unhydrated particles are formed in the morphology of the copper slag-free concrete. In this case, RCC0 has a very weak C–S–H structure and less strength than copper-slag concretes. Fig. 7B shows that increasing the curing age from 28 to 91 days will decrease the unhydrated particles as well as the lengths of ettringite pieces. In this figure, the RCC0 microstructure still has large-dimension cavities, which are important factors that reduce its strength. Previous studies have reported cavities, needle-shape ettringite structure and large amounts of unhydrated particles in the microstructure of slag-free concrete (Sharma and Khan, 2017a; Gupta and Siddique, 2019, 2020). Hydration process causes the calcium sulfate and aluminate to be separated from concrete constituents and dissolved in calcium, sulfate, hydroxyl and aluminum ions. After recombination, these ions will produce ettringite (trisulfoaluminate hydrate) and calcium hydroxide. Using the Energy Dispersive Spectroscopy (EDS) results, Gupta and Siddique (2019) attributed the formation of needle-shape ettringite particles in slag-free SCCs to aluminum and sulfur. In Fig. 7C, the 28d RCC20 morphology lacks ettringite pieces and hydration products are being formed. Here, the C–S–H has less monolithic and compact structure and contains several cavities. In this mix design, dimensions of cavities are reduced and volume of unhydrated particles is highly decreased. In fact, replacing natural aggregates with 20% CS will cause the free water to be used in the hydration process (because these wastes absorb less water than natural aggregates), leading to a decrease in the unhydrated particles and an increase in the C–S–H production. As the 91d RCC20 has enough time to complete the hydration process and benefits from sufficient moisture in the curing environment, it forms a denser and more uniform C–S–H structure and creates better quality hydration products that fill the structure cavities quite well (Fig. 7D). Presence of 40% CS in RCC40 has created a microstructure and morphology similar to those of the RCC20, but dimensions of cavities and volume of unhydrated particles have highly reduced in the 28d and 91d RCC40 compared to RCC20 (Fig. 7E–F). Reduced pore size dimension is attributed to increased hydration products and formation of more cohesive C–S–H, which have filled the pores and prevented larger unhydrated particles to form. The improved strength in this mix design is attributed to the desirable density of the produced C–S–H structure. Siddique et al. (2019) believe that the increased compressive strength of fiber concrete with 40% CS compared to the reference design is due to its improved homogeneity and microstructure. At 28 and 91 days of age, increasing the CS from 40

to 60% will create unhydrated particles, large cavities and micro-cracks in the surface morphology of the RCC60 causing its strength to decrease slightly (Fig. 7G–H). On the other hand, the copper-slag's low pozzolanic activity will cause calcium hydroxide sheets to from. In this design, after the excess water evaporates due to less water absorption of CS grains, large cavities will remain in the concrete microstructure. Contrary to the fibrous structure of the C–S–H gel in RCC0, using 60% CS has caused a relatively more integrated C–S–H gel to form on the entire surface due to its filling effect.

Some studies (Gupta and Siddique, 2019) have confirmed the presence of peaks of such elements as Ca, Si, Fe, Al, O and S in the SCC20, and some (Siddique et al., 2019) have used SEM images to show that the FRC20 structure contains calcium hydroxide (CH), calcite particles and large micro-cavities. According to Siddique et al. (2019), replacing natural fine aggregates with 40% CS in 28- and 91-day specimens will result in a more consolidated and consistent distribution of C–S–H products in the concrete matrix, and improves its microstructural quality.

Properties (shape, size, volume, surface texture, etc.) of aggregates used in the concrete production affect the ITZ specifications (quality, strength and volume fraction) which are very important when studying the concrete behavior and performance in the fracture process under tensile stresses (Akcaoglu et al., 2004). In general: 1) decreasing the aggregate size will lead to less porosity in the ITZ (due to less water accumulation around them) letting fewer cracks to pass through this area and 2) finer aggregates sense less stress due to their higher specific surface area compared to larger ones (Beygi et al., 2014). Some researches (Wu et al., 2010a; Sharma and Khan, 2017a; Rezaei Lori et al., 2019; Gupta and Siddique, 2019) have reported that more than 30% CS will reduce the concrete strength due to the formation of micro-cracks, cavities, capillary channels and ettringite particles because of the smooth glassy surface texture and low adsorption of CS aggregates that increase the free water in concrete, create micro-cracks and increase the thickness in the ITZ. The early-age cracking and stress concentration in ITZ are often attributed to the differences in the drying shrinkage and modulus of elasticity between aggregates and the cement paste (Nikbin et al., 2014). In the cement paste matrix, aggregates cause tortuosity in the fracture path causing the crack to tend to pass through weak areas such as the ITZ causing the vacuolated cement paste to increase, but when the ITZ microstructure and strength increase, the crack path should forcibly pass through the aggregates (Beygi et al., 2014).

ITZ images of concretes containing 0, 40 and 60% CS are shown in Fig. 8. In Fig. 8, the ITZ formed around (and in the vicinity of) CS aggregates shows obvious compositional and appearance differences compared to other parts of the cement matrix. It is worth noting that these differences are more pronounced near the surface texture of the CS aggregates and become insignificant at a certain distance away from the CS aggregates. As shown in Fig. 8A–D, there are numerous unhydrated particles, cavities and cracks in the ITZ of the copper slag-free design and the porosity of the ITZ layer around natural rough aggregate surfaces is higher due to their rougher surfaces compared to the copper slag. Lack of coherent, uniform C–S–H and formation of very porous heterogeneous ITZs in RCC0 will cause weak links to act as macro-crack adsorbents and provide an easier path for crack development; this phenomenon gradually evolves with interfacial micro-crack bridging. As the area around aggregates is usually known as the weakest and its concrete is important because it shows the mechanical properties of the hardened concrete, it can be concluded that the porosity, cavities and cracks in the ITZ of the RCC0 have reduced the stiffness and strength. Fig. 8E–H shows the ITZ of the RCC40; in Fig. 8H, it lacks unhydrated particles and has a more cohesive structure. However, cracks in this zone can be due to the difference in the rate of drying shrinkage and modulus of elasticity between the cement paste and CS as well as to the glass surface of these waste materials. The desirable quality and considerable cohesion of the ITZ structure in RCC40 have improved its strength and performance. On the other hand, since its ITZ lacks cavities and noticeable porosity, its durability indices have improved too. Fig. 8I-L shows different-scale ITZ images of the RCC60 design; large unhydrated particles, long cracks, low quality of hydration products and continuous capillary voids (shown in red circles/ellipses) have caused a decrease in strength and an increase in durability indices of the RCC60 compared to RCC40. Comparing Fig. 8D and L reveals that using high-volume CS compared to the "reference design" has eliminated the fibrous structure of the cement paste, created C–S–H uniformity and reduced the volume/number of cavities in the ITZ. It is worth noting that the structural/internal ITZ weaknesses (porosity, unhydrated particles, cracks, etc.) conclude that an increase in the amount or volume of this zone will increase the concrete weak points and reduce the composite strength. Compared to natural aggregates, as CS grains are more angled and broken and have higher contact surfaces with the cement paste, they create vaster and longer ITZs. Hence, increasing the CS volume up to 60% accelerates the formation and stabilizes the weaker areas in the concrete structure compared to RCC40.

Fig. 16 clearly shows how the crack-propagation direction changes when facing copper slag grains. High stiffness of CS aggregates in concrete and ITZ prevents cracks to pass through their bodies causing the fracture energy to increase, but since these aggregates are broken and angular, the fracture path becomes more winding and needs more

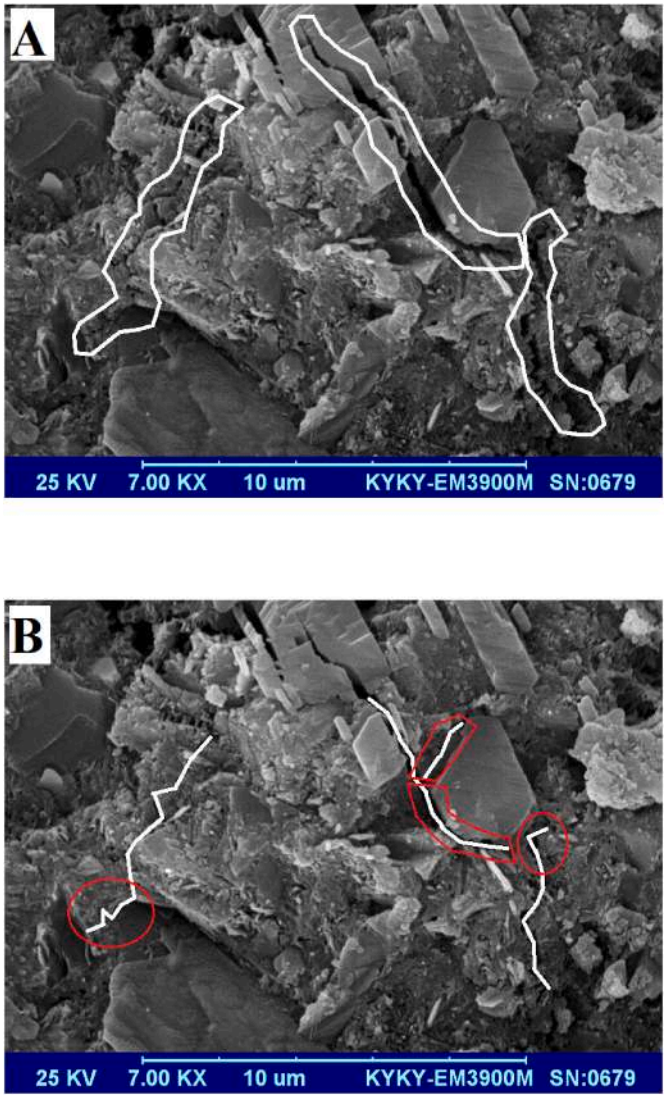

Fig. 16. Crack propagation pattern: A) Crack formation zone B) Crack propagation direction and its change when facing the CS.

energy to overcome the ITZ strength. The favorable effects of the CS on the microstructure and ITZ will increase the cement matrix resistance against the crack growth.

3.9. Economic index

Since the concrete volume used in the construction industry is considerable, using waste materials in its production, even in small amounts, can reduce the related costs. In Table 8 that shows the costs of the material purchasing, transportation and quality control of all concretes in August 2021, those of RCC10 to RCC60 show a reduction of, respectively, 4.47, 8.93, 13.41, 17.87, 22.34 and 26.80% in the production cost compared to RCC0. Replacing all fine aggregates with CS will reduce the concrete production cost by 21%; this reduction is 19% in SCCs containing coarse CS aggregates (Sharifi et al., 2020a,b). In Fig. 17, the economic index (strength/price) lies in the 0.22–0.27, 0.26–0.33 and 0.29–0.39 range for, respectively, the 7-, 28- and 91-day concretes with/without CS; that of the hardened RCC40 is the highest (considering its good performance), but in general, an increase in CS will increase the economic index of all mix designs compared to RCC0.

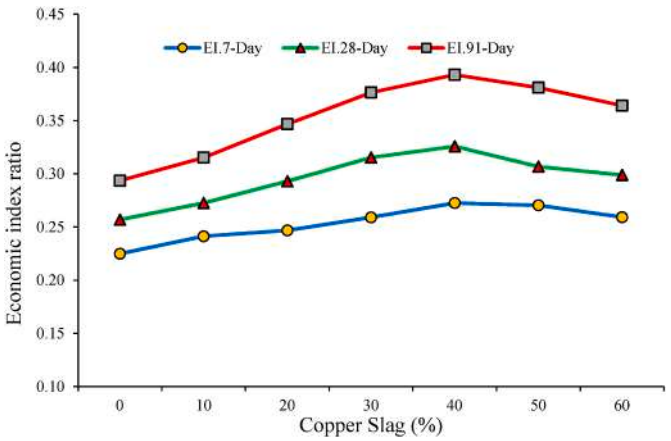

Fig. 17. The results of economic index of RCCs.

4. Conclusions

A thorough investigation and analysis of the experimental results of this study shows that if the copper slag (CS) is used in roller compacted concrete (RCC) instead of natural fine aggregates, the result will be an inexpensive, clean, green, and nature-friendly RCC. This study investigated the effects of using fine CS aggregates on the production costs, environmental merits, mechanical properties and microstructure of the RCC. To this end, 7 mix designs were prepared wherein 0, 10, 20, 30, 40, 50 and 60% CS replaced natural fine aggregates. Following are the results obtained after tests and evaluations:

1. Using 40% fine CS aggregates in 7-, 28- and 91-day RCC specimens increased the compressive strength by, respectively, 11.84, 17.01 and 23.58%. The highest flexural and tensile strengths belonged to specimens containing 60% CS at all ages due to the CS aggregates' high stiffness, angularity and breakage and, hence, a better bond with the cement paste.
2. Test results revealed that increasing fine CS aggregates in the RCC by up to 40% reduced the surface and capillary water-absorption rates compared to the control design. The surface absorption rate of all 91-day specimens, with/without CS, was less than 7% and RCC60 had a 56% reduction in capillary water absorption compared to RCC0.
3. In general, 0–60% CS reduced the water penetration depth in RCC specimens; at 40%, the penetration depth reduced by about 38.5% compared to RCC0 due, maybe, to the increased and improved hydration products, reduced pores and disconnection of voids.
4. SEM images revealed that voids, micro-cracks, un-hydrated particles and ettringite reduced the concrete strength with/without CS. Replacing 40% natural fine aggregates with CS produced a dense and homogeneous C–S–H gel structure and improved the strength.
5. Using 60% fine CS aggregates in producing green RCCs reduced the construction costs by 26.8% - a significant savings in bulk concreting. The high RCC40 strength caused its economic index (strength/price) to be higher than that of all other mix designs.
6. Using CS waste fine aggregates in producing the RCC will not only prevent environmental problems, eliminate the need for depots, reduce the energy consumption and enhance the sustainable development, but will also result in the production of clean, inexpensive, nature-friendly concretes.
7. Considering the environmental concepts, using 60% (maximum) CS is quite satisfactory and can highly reduce the depot-caused damage of this waste material. However, based on the results of mechanical tests, evaluation of durability indices, comparison of economic indices and positive effects of using 40% CS (as fine aggregates) on reducing the environmental problems of this waste material, the mix design containing 40% CS (RCC40) is introduced as the optimal design

Suggestions for future studies

Future studies need, for this type of concrete, to study and evaluate: 1) fracture parameters under different loading modes, 2) strength against heat, 3) performance in acidic environments, 4) electrical resistance, 5) effects of carbonation and 6) thaw/freeze cycles.

CRediT authorship contribution statement

Ehsan Sheikh: Writing – original draft, Data curation, Writing – original draft, preparation. **Seyed Roohollah Mousavi:** Conceptualization, Methodology, Investigation, Reviewing and Editing, Supervision, Project administration, Funding acquisition. **Iman Afshoon:** Resources, Methodology, Formal analysis, Writing – original draft, Data curation, Writing – original draft, preparation, Software.

Declaration of competing interest

The authors declare that they have no known competing financial interests or personal relationships that could have appeared to influence

Table 8
Cost analysis of RCCs.

Material	Cost ($/Kg)	Mix Description						
		RCC0	RCC10	RCC20	RCC30	RCC40	RCC50	RCC60
OPC (Kg)	0.09	24.85	24.85	24.85	24.85	24.85	24.85	24.85
FA (Kg)	0.058	55.95	50.35	44.76	39.16	33.57	27.97	22.38
CA (Kg)	0.039	40.88	40.88	40.88	40.88	40.88	40.88	40.88
CS (Kg)	0.0016	0.00	0.16	0.32	0.47	0.63	0.79	0.95
Water (Kg)	0.0003125	0.034	0.034	0.034	0.034	0.034	0.034	0.034
Total		121.71	116.28	110.84	105.40	99.97	94.53	89.09

the work reported in this paper.

References

Achudhan, Deepavarsa, Vandhana, Khalida, 2018. Effect of copper slag in structural behavior of reinforced concrete beams. Mater. Today Proc. 5, 6878–6887.

ACI: 325.10R-95, 2001. State of Art Report on Roller Compacted Concrete Pavements. American Concrete Institute Report.

Afshoon, I., Sharifi, Y., 2014. Ground copper slag as a supplementary cementing material and its influence on the fresh properties of self-consolidating concrete. IES J. Part A Civ. Struct. Eng. 7, 229–242.

Afshoon, I., Sharifi, Y., 2017. Use of copper slag microparticles in self-consolidating concrete. ACI Mater. J. 5, 114.

Afshoon, I., Sharifi, Y., 2020. Utilization of micro copper slag in SCC subjected to high temperature. J. Build. Eng. 29, 1011–1028.

Akcaoglu, T., Tokyay, M., Celik, T., 2004. Effect of coarse aggregate size and matrix quality on ITZ and failure behavior of concrete under uniaxial compression. Cem. Concr. Compos. 26, 633–638.

Al-Jabri, K.S., Hisada, M., Al-Saidy, A.H., Al-Oraimi, S.K., 2009a. Performance of high strength concrete made with copper slag as a fine aggregate. Construct. Build. Mater. 23, 2132–2140.

Al-Jabri, K.S., Hisada, M., Al-Oraimi, S.K., Al-Saidy, A.H., 2009b. Copper slag as sand replacement for high performance concrete. Cement Concr. Compos. 31, 483–488.

Al-Jabri, K.S., Al-Saidy, A.H., Taha, R., 2011. Effect of copper slag as a fine aggregate on the properties of cement mortars and concrete. Construct. Build. Mater. 25, 933–938.

Ali Ahmad, M., Miri, M., Rashki, M., 2017. Probabilistic and experimental investigating the effect of pozzolan and Lumachelle fine aggregates on roller compacted concrete properties. Construct. Build. Mater. 151, 755–766.

Ambily, P.S., Umarani, C., Ravisankar, K., Prem, P.R., Bharatkumar, B.H., Iyer, N.R., 2015. Studies on ultra-high performance concrete incorporating copper slag as fine aggregate. Construct. Build. Mater. 77, 233–240.

Arino, A.M., Mobasher, B., 1999. Effect of ground copper slag on strength and toughness of cementitious mixes. ACI Mater. J. 96 (1), 68–73.

Association, E.A., 2018. Estimates of aggregates production Data. Available from. www.uepg.eu/statistics/estimates-of-production-data/data-2015.

ASTM C 1252 – 03, 2003. Standard Test Methods for Un-compacted Void Content of Fine Aggregate (As Influenced by Particle Shape, Surface Texture, and Grading).

ASTM C 127-07, 2007. Standard Test Method for Density, Relative Density (Specifc Gravity), and Absorption of Coarse Aggregate. ASTM International.

ASTM C 128-07, 2007. Test Method for Density, Relative Density (Specifc Gravity), and Absorption of Fine Aggregate. ASTM International.

ASTM C 1435 – 08, 2008. Standard Practice for Molding Roller-Compacted Concrete in Cylinder Molds Using a Vibrating Hammer. ASTM International.

ASTM C 150M-09, 2009. Standard Specifcation for Portland Cement. ASTM International.

ASTM C 1585-04, 2004. Standard Test Method for Measurement of Rate of Absorption of Water by Hydraulic-Cement Concretes. ASTM International.

ASTM C 33M-08, 2008. Standard Specifcation for Concrete Aggregates. ASTM International.

ASTM C 39M – 09, 2009. Standard Test Method for Compressive Strength of Cylindrical Concrete Specimens. ASTM International.

ASTM C 496M-04, 2004. Standard Test Method for Splitting Tensile Strength of Cylindrical Concrete Specimens. ASTM International.

ASTM C 642-06, 2006. Standard Test Method for Density, Absorption, and Voids in Hardened Concrete. ASTM International.

Beygi, H.A., Kazemi, M., Nikbin, M., M, T., Vaseghi Amiri, I., Rabbanifa, J., Rahmani, S., 2014. The influence of coarse aggregate size and volume on the fracture behavior and brittleness of self-compacting concrete. Cement Concr. Res. 66, 75–90.

Boakye, D.M., Uzoegbo, H.C., 2014. Durability and Strength Assessment of Copper Slag Concrete. RILEM International Workshop on Performance-Based Specification and Control of Concrete Durability, Zagreb, Croatia, pp. 647–654.

ASTM C 1690M-12, 2012. Standard Test Method for Flexural Performance of Fiber Reinforced Concrete (Using Beam with Third-point Loading). ASTM International.

ASTM C 29M-09, 2009. Standard Test Method for Bulk Density (“Unit Weight”) and Voids in Aggregate. ASTM International.

ASTM C 78-09, 2009. Standard Test Method for Flexural Strength of Concrete (Using Simple Beam with Third-point Loading). ASTM International.

ASTM C 94M-09, 2009. Standard Specifcation for Ready – Mixed Concrete. ASTM International.

Iranian code 354, 2009. Guidelines for the Design and Construction of Roller-Compacted Concrete Pavements, Ministry of Roads and Transportation Deputy of Training; Research and Information Technology. http://seso.moe.org.ir.

Dhar, A., Rajasankar, J., Anandavalli, N., 2018. A mathematical formulation to find effective bulk and shear moduli of recycled aggregate concrete. Construct. Build. Mater. 168, 747–757.

BS EN 12390, 2009. Testing Hardened Concrete: Density of Hardened Concrete. Part 7. CEB-FIB, 1993. CEB-FIP Model Code 1990. Committee Euro-International du Beton, Lausanne, Switzerland.

BS EN12390-8, 2000. Testing Hardened Concrete.Depth of Penetration of Water under Pressure.

Fakhri, M., Saberi, F., 2016. The effect of waste rubber particles and silica fume on the mechanical properties of Roller Compacted Concrete Pavement. J. Clean. Prod. 129, 521–530.

Freedonia, 2012. World Construction Aggregates, Industry Study No. 2838. The Freedonia Group, Cleveland, Ohio, USA.

Gesoglu, H.M., Güneyisi, E., Mahmood, S.F., 2016. Combined use of natural and artificial slag aggregates in producing self-consolidating concrete. ACI Mater. J. 113 (5), 599.

Gharavi, M., 2003. Optimization of compacting time with the effects of different pozzolans (type and dosage) on the mechanical properties of RCC. In: Fourth International Symposium on Roller Compacted Concrete (RCC) Dams. Madrid, Spain.

Gorai, B., Jana, R.K., Premchand, 2003. Characteristics and utilization of copper slag - a review. Resour. Conserv. Recycl. 39, 299–313.

Gupta, N., Siddique, R., 2019. Strength and micro-structural properties of self-compacting concrete incorporating copper slag. Construct. Build. Mater. 224, 894–908.

Gupta, N., Siddique, R., 2020. Durability characteristics of self-compacting concrete made with copper slag. Construct. Build. Mater. 247, 118580.

Hall, C., 1989. Water sorptivity of mortars and concretes: a review. Mag. Concr. Res. 41, 51–61.

IEA, WBCSD, 2009. Cement Technology Roadmap. Carbon Emissions Reductions up to 2050. International Energy Agency. World Business Council for Sustainable Development, Paris, France.

Karimpour, A., 2010. Effect of time span between mixing and compacting on roller compacted concrete (RCC) containing ground granulated blast furnace slag (GGBFS). Construct. Build. Mater. 24, 2079–2083.

Khanzadi, M., Behnood, A., 2009. Mechanical properties of high-strength concrete incorporating copper slag as coarse aggregate. Construct. Build. Mater. 23, 2183–2188.

Liu, D.H., Li, Z.L., Liu, J.L., 2015. Experimental study on real-time control of roller compacted concrete dam compaction quality using unit compaction energy indices. Construct. Build. Mater. 96, 567–575.

Mirhosseini, S.R., Fadaee, M., Tabatabaei, R., Fadaee, M.J., 2017. Mechanical properties of concrete with Sarcheshmeh mineral complex copper slag as a part of cementitious materials. Construct. Build. Mater. 134, 44–49.

Mobasher, B., Devaguptapu, R., Arino, A.M., 1996. Effect of copper slag on the hydration of blended cementitious mixtures. In: Chong, K. (Ed.), Proceedings, ASCE, Materials Engineering Conference, Materials for the New Millennium, pp. 1677–1686.

Modarres, A., Hosseini, Z., 2014. Mechanical properties of roller compacted concrete containing rice husk ash with original and recycled asphalt pavement material. Mater. Des. 64, 227–236.

Mousavi, S.R., Afshoon, I., Bayatpour, M.A., Davarpanah, A.H., Miri, M., 2021. Effect of waste glass and curing aging on fracture toughness of self-compacting mortars using ENDB specimen. Construct. Build. Mater. 282, 122711.

Najimi, M., Sobhani, J., Pourkhorshidi, A.R., 2011. Durability of copper slag contained concrete exposed to sulfate attack. Construct. Build. Mater. 25, 1895–1905.

Nazer, A., Borrachero, J.P.M.V., Monzo, J., 2016. Use of ancient copper slags in Portland cement and alkali activated cement matrices. J. Environ. Manag. 167, 115–123.

NEAPRC, 2009. National Energy Administration of People’s Republic of China, Construction Specifications for Hydraulic RCC (DL/T 5112–2009). Water Power Press, Beijing (in Chinese).

Nematollahzade, M., Tajadini, A., Afshoon, I., Aslani, F., 2020. Influence of different curing conditions and water to cement ratio on properties of self-compacting concretes. Construct. Build. Mater. 237, 117570.

Nikbin, M., I, Beygi, M.H.A., Kazemi, M.T., Vaseghi Amiri, J., Rahmani, E., Rabbanifar, S., Eslami, M., 2014. Effect of coarse aggregate volume on fracture behavior of self-compacting concrete. Construct. Build. Mater. 52, 137–145.

Obe, R.K.D., Brito, D.J., Mangabhai, R., Lye, C.Q., 2016. Sustainable Construction Materials: Copper Slag. Woodhead Publishing.

Ong, B.S., 2009. Study of Concrete Containing Washed Copper Slag. School of Civil and Environmental Engineering: Nanyang Technological University [Final Year Project].

Prem, P.R., Verma, M., Ambily, P.S., 2018. Sustainable cleaner production of concrete with high volume copper slag. J. Clean. Prod. 193, 43–58.

Rajasekar, A., Arunachalam, K., Kottaisamy, M., 2019. Assessment of strength and durability characteristics of copper slag incorporated ultra-high strength concrete. J. Clean. Prod. 208, 402–414.

Rao, S.K., Sravana, P., Rao, T.C., 2016. Abrasion resistance and mechanical properties of roller compacted concrete with GGBS. Construct. Build. Mater. 114, 925–933.

Rezaei Lori, A., Hassani, A., Sedghi, R., 2019. Investigating the mechanical and hydraulic characteristics of pervious concrete containing copper slag as coarse aggregate. Construct. Build. Mater. 197, 130–142.

Rooholamini, H., Sedghi, R., Ghobadipour, B., Adresi, M., 2019. Effect of electric arc furnace steel slag on the mechanical and fracture properties of roller-compacted concrete. Construct. Build. Mater. 211, 88–98.

Samimi, K., Kamali-Bernard, S., Maghsoudi, A.A., Maghsoudi, M., Siad, H., 2017. Influence of pumice and zeolite on compressive strength, transport properties and resistance to chloride penetration of high strength self-compacting concretes. Construct. Build. Mater. 151, 292–311.

Sharifi, Y., Afshoon, I., Firoozjaei, Z., 2015. Fresh properties of self-compacting concrete containing ground waste glass micro-particles as cementing material. J. Adv. Con. Technol. 13 (2), 50–66.

Sharifi, Y., Afshoon, I., Firoozjaei, Z., Momeni, M., 2016. Utilization of waste glass micro-particles in producing self-consolidating concrete mixtures. Int. J. Concr. Struct. Mater. 10 (3), 337–353.

Sharifi, Y., Afshoon, I., Asad-Abadi, S., Aslani, F., 2020a. Environmental protection by using waste copper slag as a coarse aggregate in self-compacting concrete. J. Environ. Manag. 271, 111013.

Sharifi, Y., Afshoon, I., Nematollahzade, M., Ghasemi, M., Momeni, M., 2020b. Effect of copper slag on the resistance characteristics of SCC exposed to the acidic environment. Asian J. Civ. Eng. 21, 597–609.
Sharma, R., Khan, R.A., 2017a. Fresh and mechanical properties of self-compacting concrete containing copper slag as fine aggregates. J. Mater. Eng. Struc. 4, 25–36.
Sharma, R., Khan, R.A., 2017b. Sustainable use of copper slag in self compacting concrete containing supplementary cementitious materials. J. Clean. Prod. 151, 179–192.
Sharma, R., Khan, R.A., 2017c. Durability assessment of self-compacting concrete incorporating copper slag as fine aggregates. Construct. Build. Mater. 155, 617–629.
Sharma, R., Khan, R.A., 2018. Influence of copper slag and metakaolin on the durability of self- compacting concrete. J. Clean. Prod. 171, 1171–1186.
Shen, H., Forssberg, E., 2003. An overview of recovery of metals from slags. Waste Manag. 23, 933–949.
Shi, C., Meyer, C., Behnood, A., 2008. Utilization of copper slag in cement and concrete. Resour. Conserv. Recycl. 52, 1115–1120.
Siad, H., 2010. Influence of the Type of Mineral Addition on the Physical and Mechanical Behavior and Durability of Self-Compacting Concrete [Dissertation]. INSA de Rennes, France.
Siddique, R., Singh, M., Jain, M., 2019. Recycling copper slag in steel fibre concrete for sustainable construction. J. Clean. Prod. 271, 122559.
Singh, G., Siddique, R., 2016. Strength properties and micro-structural analysis of self-compacting concrete made with iron slag as partial replacement of fine aggregates. Construct. Build. Mater. 127, 144–152.
Vijayaraghavan, J., Belin Judeb, B., Thivya, J., 2017. Effect of copper slag, iron slag and recycled concrete aggregate on the mechanical properties of concrete. Resour. Pol. 53, 219–225.
Wang, X.h., Zhang, S.R., Wang, C., Liu, F.C., Song, R., Wei, P.y., 2018. Initial damage effect on dynamic compressive behaviors of roller compacted concrete (RCC) under impact loadings. Construct. Build. Mater. 186, 388–399.
Wu, W., Zhang, W., Ma, Q., 2010a. Optimum content of copper slag as fine aggregate in high strength concrete. Mater. Des. 31, 2878–2883.
Wu, W., Zhang, W., Ma, Q., 2010b. Mechanical properties of copper slag reinforced concrete under dynamic compression. Construct. Build. Mater. 24, 910–917.

Glossary

Acronyms

CS: Copper slag
RCC: roller compacted concrete
SEM: scanning electron microscope
RHA: rice husk ash
EAF: electric arc furnace
SCC: self-compacting concrete
HSC: high strength concrete
RC: reinforced concrete
UPV: Ultrasonic pulse velocity
EDS: energy dispersive spectroscopy
HPC: high-performance concretes
SSD: saturated surface dry
C–S–H: calcium silicate hydrate
ITZ: interfacial transition zone
EI: economic index (strength/price)
OPC: ordinary portland cement
FA: fine aggregate
CA: coarse aggregate
SFRC: steel fiber reinforced concrete Symbols
W/C: water to cement ratio
WS: mass of oven-dried sample in air (gr)
WD: mass of surface-dry sample in air after immersion (gr)
K: sorptivity coefficient ($cm/s^{0.5}$)
Q: absorbed water (cm3)
A: section area (cm^2)
T time (s): F_c compressive strength (MPa)
F_{c28}: compressive strength (MPa) of the 28-day
RCC0: F_t split strength (MPa)
F_{t28}: split strength (MPa) of the 28-day RCC0
F_r: flexural strength (MPa)
F_{r28}: flexural strength (MPa) of the 28-day RCC0